Estuarine, Coastal and Shelf Science (1995) **40,** 505–528

Entrainment of Nitrate in the Fraser River Estuary and its Biological Implications. I. Effects of the Salt Wedge

Kedong Yin[a], Paul J. Harrison[a], Stephen Pond[a] and Richard J. Beamish[b]

[a]*Department of Oceanography, University of British Columbia, Vancouver, British Columbia, V6T 1Z4 Canada and* [b]*Pacific Biological Station, Department of Fisheries and Oceans, Nanaimo, British Columbia, V9R 5K6 Canada*

Received 2 December 1992 and in revised form 14 April 1994

Keywords: nitrate entrainment, chlorophyll maximum; salt wedge; riverine plume; estuarine plume; tides; river discharge; Fraser River; Canada west coast

A series of high-resolution vertical profiles of temperature, salinity, NO_3 and fluorescence were taken along a transect of the Fraser River estuary to investigate entrainment of NO_3. In late spring and summer, the NO_3-poor estuarine plume was found to invade the river with the advancing salt wedge on the flood tide and to form a middle layer between the river water and the NO_3-rich deep seawater in the salt wedge, forming a three-layered system. Thus, during entrainment the upward flux of salt into the riverine plume does not necessarily result in an upward flux of NO_3 due to the entrainment of low NO_3 estuarine plume water. Therefore, the amount of the entrained NO_3 was determined by the amount of the entrained deep water. Entrainment was affected by the tides, with more entrainment occurring during spring than neap tides. At lower low water during a spring tide, the river outflow was stronger and it pushed the estuarine plume water seaward more effectively. Thus, the outflowing freshwater entrained more NO_3-rich deep water during spring tides. There was a chlorophyll maximum located at the bottom of the interface between the estuarine plume and the deep water. The maximum was advected into the river with the invasion of the incoming salt wedge on flood tides and entrained into the outflowing riverine plume on tidal ebbs. The chlorophyll maximum under the riverine plume was often below the euphotic zone and little uptake of nutrients occurred in the dark in samples taken from it at the time of sampling. However, when the samples were incubated under different irradiances, uptake of nutrients increased with increasing irradiance. Thus the phytoplankton in the chlorophyll maximum could serve as a potential seed population for blooms in regions further seaward beyond the river mouth when they were entrained into a zone with improved irradiance and entrained nutrients.

Introduction

Entrainment is one of the principal physical processes that causes the transfer of salt water into the freshwater in an estuary. It usually occurs when a surface freshwater layer

0272–7714/95/050505+24 $08/00/0

flows over a layer of salt water underneath and the velocity shear between the two layers is sufficiently strong. The shear instability can be observed with an echo sounder (Brandt *et al.*, 1987; Geyer & Farmer, 1989). During the process of upward entrainment in estuaries, salinity increases in the surface layer. The resulting concentration of nutrients, however, depends on the concentrations of source nutrients. When the river has a lower nutrient concentration than the seawater, entrainment will result in an increase in concentration of that nutrient with salinity in the surface layer; if the river has higher nutrient concentrations, entrainment of the seawater results in a dilution. Entrainment is an important process in mixing nutrients to the surface layer. In the St Lawrence estuary, intensive entrainment occurs at the head of the Laurentian Channel (Ingram, 1979). This entrainment is suggested to play an important role in nutrient supply, by acting as a ' nutrient pump ' and enhancing biological production in the Gaspé Current (Steven, 1974). There are few quantitative studies on the dynamics of nutrients associated with mixing processes caused by entrainment (Mann & Lazier, 1991).

The Fraser River discharge starts to increase in March, reaches a maximum (up to 10 000 $m^3 s^{-1}$) in June, gradually decreases in July, August and September, and then remains near the minimum levels (down to 700 $m^3 s^{-1}$) throughout the rest of the year. From March to September, the discharged freshwater is mixed with seawater in the Strait of Georgia and most of the mixture remains in the Strait of Georgia, forming a stratified water body which is referred to as the estuarine plume (Harrison *et al.*, 1991). The surface salinity in the estuarine plume ranges from 15 to 25. The bottom boundary of the estuarine plume can be approximately defined by a salinity of 28 at a depth of 19–20 m in late spring and summer. The estuarine plume extends over most of the central and southern regions of the Strait (Waldichuk, 1957). Because the estuarine plume is a stratified water column, nutrients (inorganic nitrogen) are often undetectable during this period (Clifford *et al.*, 1989, 1990, 1991; Harrison *et al.*, 1991).

The daily freshwater outflow in the Fraser River is tidally modulated, being dammed during tidal floods, and released during tidal ebbs. A salt wedge invades the river during tidal floods and retreats during tidal ebbs. Upward entrainment of salt water into the freshwater occurs mostly during tidal ebbs (Geyer & Farmer, 1989). The movement of the salt wedge in the river depends on tides and the magnitude of the river discharge (Kostaschuk & Atwood, 1989). When the Fraser River outflow is released during ebb tides, it forms the riverine plume in the Strait which spreads over the estuarine plume. The surface salinity of the riverine plume ranges from 0 near the river mouth to 15 seaward depending on how much seawater is entrained. The surface horizontal boundary of the riverine plume is a riverine front and the vertical extent is usually bounded by a sharp halocline in the top 5 m. Thus, both plumes entrain salt, with the riverine plume usually entraining salt from the estuarine plume and the latter entraining the deeper seawater below. In late spring and summer, little NO_3 will be entrained from the estuarine plume into the riverine plume. Horizontal mapping of salinity and vertical salinity and nutrient profiles clearly showed the two plumes in the water column based on two distinct sharp haloclines (Harrison *et al.*, 1991). Nitrate was frequently undetectable in the estuarine plume and was observed as a minimum zone at an intermediate depth in the vertical profile when the riverine plume spread over the estuarine plume. The entrainment from the estuarine plume to the riverine plume results in an increase in salinity but a decrease in concentration of NO_3 in the riverine plume compared to the river.

Estimates of entrainment of salt in the Strait of Georgia due to the Fraser River runoff have been made (Cordes *et al.*, 1980). However, such an estimate based on salt conservation without knowledge of the nutrient concentrations does not allow an estimate of the entrainment of nutrients.

The Fraser River is one of the largest rivers along the west coast of North America. Its discharge contributes 85% of the runoff into the Strait of Georgia (Waldichuk, 1957). Nitrate concentrations in the river also change seasonally, with the highest values in February (*c.* 14 μM) and the lowest in August (down to 2 μM) (Drinnan & Clark, 1980). Entrainment has been proposed to be the main process which supplies nitrate for primary productivity in late spring and summer (Parsons *et al.*, 1980; Harrison *et al.*, 1983). So far, no quantitative study of the entrainment of nutrients has been made for the Strait of Georgia.

This study examined the entrainment process along a transect in the Fraser River estuary. The objectives of this study were: (1) to investigate if the NO_3-poor estuarine plume (summer months) invades the river with the salt wedge on the flood tides and becomes a barrier to nutrient entrainment by the surface waters since it lies between the river and the NO_3-rich deep seawater; (2) to determine if entrainment of NO_3 takes place in association with mixing processes; (3) to determine the effects of tides on entrainment; and (4) to investigate the biological significance of the entrainment. This study also provides some background and observational data for the subsequent two papers in which we will examine entrainment of NO_3 at an anchored station near the river mouth under spring/neap tidal conditions and different magnitudes of river discharge (Yin *et al.*, 1995*a*) and under different wind conditions (Yin *et al.*, 1995*b*).

Materials and methods

This study is part of a larger project that was conducted in 5 successive years from 1987–1991, covering most of central part of the Strait of Georgia and the lower estuary of the Fraser River, in order to investigate the dynamics of nutrients, phytoplankton productivity, and zooplankton.

Vertical profiling system

An InterOcean CTD was used to measure depth, temperature and salinity during the 1989 cruise. During the 1991 cruise, an InterOcean S4 was used to measure the same parameters plus current velocity. An opaque rubber hose was attached to the instruments and was connected with a Moyno pump on deck. Water was pumped to a fluorometer (Turner Designs) to measure *in vivo* fluorescence and to an AutoAnalyzer to measure nutrients. This system could produce continuous vertical profiles (to 25 m) of current velocity, temperature, salinity, density, fluorescence and nutrient concentrations while the S4 or CTD was lowered slowly (*c.* 1 m min^{-1}) through the water column. Data were recorded by a computer. The travel time of water through the hose and the AutoAnalyzer system was carefully measured and considered in the computer program in order to adjust for the differences in response time between different parameters. Nutrient concentrations in vertical profiles were corrected for baseline drift. Additional details on the system are published elsewhere (Jones *et al.*, 1991). Data from a vertical profile were smoothed over 0·5-min intervals. This smoothing reduced the fluctuations caused by the ship's motion.

Nutrient analysis

Nitrate (plus nitrite) and ammonium were determined following the procedures of Wood *et al.* (1967) and Slawyk and MacIsaac (1972), respectively. Silicate and phosphate were analysed according to Armstrong *et al.* (1967) and Hager *et al.* (1968), respectively.

Uptake experiment

Uptake experiments were conducted by taking a water sample at the depth of the chlorophyll *a* maximum and incubating on deck a subsample at different irradiances ranging from darkness and 1–100% surface light. The different irradiances were achieved by placing various layers of neutral density screen over the incubated samples which were cooled with flowing surface seawater. During the 9-h incubation period, nutrient concentrations were measured at the beginning, middle and end of the incubation. Thus, two uptake rates were obtained for each nutrient and averaged.

Tides, river discharge and winds

Observed hourly tidal heights were provided by the Tides and Current Section, Institute of Ocean Sciences, Sidney, British Columbia. The discharge data for the Fraser River at Hope were obtained from the Water Survey of Canada. The wind data were recorded at the Vancouver International Airport and provided by Atmospheric Environment Service, Environment Canada.

Temperature–salinity diagram

Temperature–salinity (T-S) diagrams were frequently used to distinguish three water masses: the riverine plume, the estuarine plume and the deep seawater below the estuarine plume. When two water types A and B with different salinity and temperature are mixed in any proportion, the resulting water type C with a new salinity and temperature will be on the straight line between A and B. From the distance of C to A or B, the proportion of A and B in C can be calculated. Similarly, if three water types (A, B and C) are mixed in any proportion, the resulting water type will be within the triangle formed by A, B and C. The relative proportions of each type can be calculated according to equations (1), (2) and (3) as follows.

One T-S diagram can be produced from one vertical profile. All the T-S diagrams of vertical profiles that were sampled during one transect, or one time series made within 24 h were plotted in one graph (e.g. Figure 1). Then the following procedures were used: Temperature and salinity in the river were plotted as ($S1$, $T1$) = (0, $T1$) where $T1$ is directly measured. 0, $T1$ are the characteristic S and T values for the river. A maximum salinity and a minimum temperature were obtained from the graph as the characteristic S and T of the deep seawater ($S3$ and $T3$) (usually this is a point at the lowest end of a T-S line). The characteristic S and T of the estuarine plume ($S2$, $T2$) were determined by extrapolating the linear trend in the outer edge of the graph, forming a triangular envelope as shown in Figure 1. The equations for conservation of salinity, temperature and volume are (Pickard & Emery, 1982):

$$V1*T1 + V2*T2 + V3*T3 = T_i \quad (1)$$

$$V1*S1 + V2*S2 + V3*S3 = S_i \quad (2)$$

$$V1 + V2 + V3 = 1 \quad (3)$$

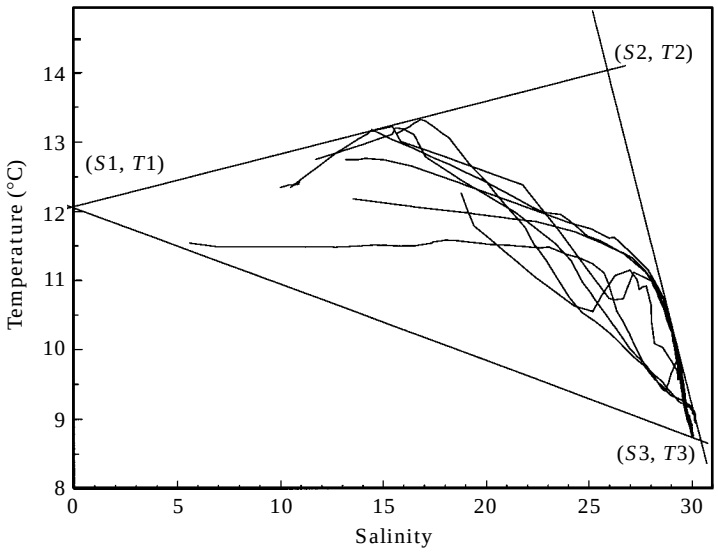

Figure 1. Temperature–salinity diagrams from a time series of vertical profiles taken on 31 May–1 June 1990 were plotted on one graph to determine the characteristic salinity and temperature ($S2$, $T2$). The same procedure was used for the transect sampled on 7–8 August 1991.

where T_i and S_i are the measured temperature and salinity values, respectively, at a depth (D_i) in a vertical profile as shown in Figure 2(a), and $V1$, $V2$ and $V3$ are the relative proportions per unit of water volume (1 m^3) of freshwater, the estuarine plume and the deep seawater with S_i and T_i at D_i, respectively. The relative proportions ($V1_i$, $V2_i$ and $V3_i$) of the three water types were calculated at D_i by solving the three equations.

At some depth, D_0 [Figure 2(b)], at which $V1$ (freshwater proportion) equals 0, $V1$, $V2$ and $V3$ were vertically integrated over depth to D_0 as in the following equation: for example, an equivalent thickness of freshwater equals

$$\sum_{D_i=0}^{D_0} \frac{(V1_i + V1_{i+1})}{2} * (D_{i+1} - D_i)$$

The same calculations were done for the $V2$ and $V3$. The integrated values are the equivalent thickness of the freshwater, the entrained estuarine plume (EEP) and the entrained deep seawater (EDW), respectively. The sum of three equivalent thicknesses is the depth of freshwater penetration (D_0). An equivalent thickness is like compacting each water type distributed over depth in a water column into one layer (in m). This layer's thickness represents the volume contributed by this water type in the water column. The equivalent thickness of the estuarine plume (EP) is obtained by integrating a proportion of it over the entire water column instead of D_0. The method for calculating the equivalent thickness of different water types in the water column is basically according to Pickard and Emery (1982).

The amount of entrained NO_3 (Ent. NO_3) is defined as the amount of NO_3 in the water column minus the contribution of river-borne NO_3 above the freshwater penetration depth D_0. Thus,

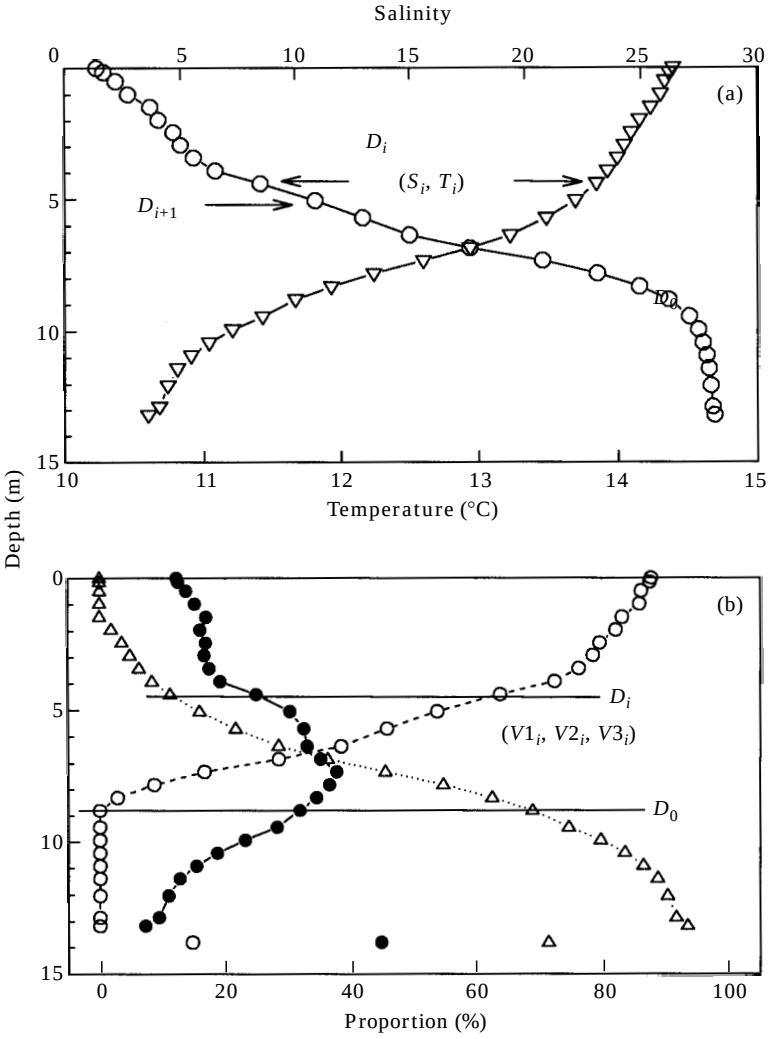

Figure 2. (a) Vertical profiles of salinity (—○—) and temperature (—▽—) showing a depth D_i at which salinity and temperature are S_i, T_i; (b) the vertical distribution of proportion of freshwater (FW), the estuarine plume (EP), and the deep water (DW) calculated from equations (1), (2) and (3) in the text, showing the calculated proportion $V1_i$, $V2_i$ and $V3_i$ at D_i for FW (- - ○ - -), EP (—●—) and DW (· ·△· ·), respectively. Integrating $V1$, $V2$ and $V3$ over depth to D_0 is the equivalent thickness of FW, the entrained estuarine plume (EEP) and the entrained deep water (EDW), respectively.

$$\text{Ent. } NO_3 = \sum_{D_i=0}^{D_0} \left(\frac{C_i + C_{i+1}}{2} - Cr \frac{V1_i + V1_{i+1}}{2} \right) * (D_{i+1} - D_i)$$

where C_i is the measured concentration at D_i in a vertical profile of NO_3; Cr is the concentration in freshwater, and $V1_i$ is the proportion of freshwater at D_i ($Cr*V1_i$ is the concentration contributed by freshwater to the measured NO_3 concentration).

The integrated fluorescence (Int. Flu.) in the water column contributed by the proportion of the estuarine plume is calculated by the following integration:

$$\text{Int. Flu.} = \sum_{D_i=0}^{20m} \frac{V2_i * F_i + V1_{i+1} * F_{i+1}}{2} * (D_{i+1} - D_i)$$

If mixing processes dominate biological processes in distributing fluorescence in the water column, a correlation between Int. Flu. and the equivalent thickness of the estuarine plume along a transect or over a time series (note: a vertical profile only produces a pair of Int. Flu. and EP) should exist.

The Practical Salinity Scale is used in the context of text and figures for salinity measurement. Therefore, the salinity values have no units, but they are equivalent to ‰ (Pond & Pickard, 1978).

Conceptual model

Our results below clearly demonstrate the presence of three water masses in the Fraser River estuary: the riverine plume, the estuarine plume and deep water. The mixing among them and the entrainment of NO_3 are controlled by tides and river discharge. Based on previous studies (Stronach, 1981; Ages & Wollard, 1988; Geyer & Farmer, 1989) and this study, a conceptual model is put forward to describe the processes of entrainment associated with the dynamics of the salt wedge as shown in Figure 3.

During a flood tide, the salt wedge invades the river at depth. The outflow of the freshwater layer slows down (Geyer & Farmer, 1989). By the end of the flood tide, the river outflow can be completely damned. The estuarine plume is pushed up at the river mouth and can be pushed into the river at the surface [Figure 3(a)]. Little upward mixing takes place during the advance of the salt wedge although downward entrainment occurs (Geyer & Farmer, 1989).

During a tidal ebb, three distinct phases of the flow can be recognized (Geyer & Farmer, 1989). In the first phase, the surface flow starts to increase downstream while the salt wedge remains stagnant. There is little mixing between the freshwater layer and the lower water layer during this phase. In the second phase, the salt wedge starts to retreat as the tidal level falls. Intensive entertainment takes place between the two layers. As a result, the halocline broadens (as viewed in a vertical profile). At the same time, the freshwater layer becomes thicker and the bottom mixed layer in the salt wedge becomes thinner. This process may lead eventually to the collapse of the salt wedge in the last phase (Ages & Woollard, 1988; Geyer & Farmer, 1989). After the salt wedge is broken down and swept out of the Fraser River, a wall of high-salinity water is formed at the river mouth [Figure 3(b)] (Stronach, 1981; Geyer & Farmer 1989; Kostaschuk & Atwood, 1989). When the river outflow hits this wall, it will move over it and entrain deep water from it. The area of this wall exposed to the riverine plume depends on both tidal levels and river discharge rate. Also, the area and NO_3 concentration in the seawater wall affect the amount of NO_3 entrained.

Results and discussion

The study area and stations with their depths are shown in Figure 4. The end of the jetty extending into the Strait is called Sand Heads and is considered to be the mouth of the river. Note that the depth beyond this jetty sharply drops from 15 to 200 m within 8 km. Stations along a transect at R1, R2, R3, R4, R5, R6, R7 and station 2 were sampled for vertical profiles on 13–14 August 1991.

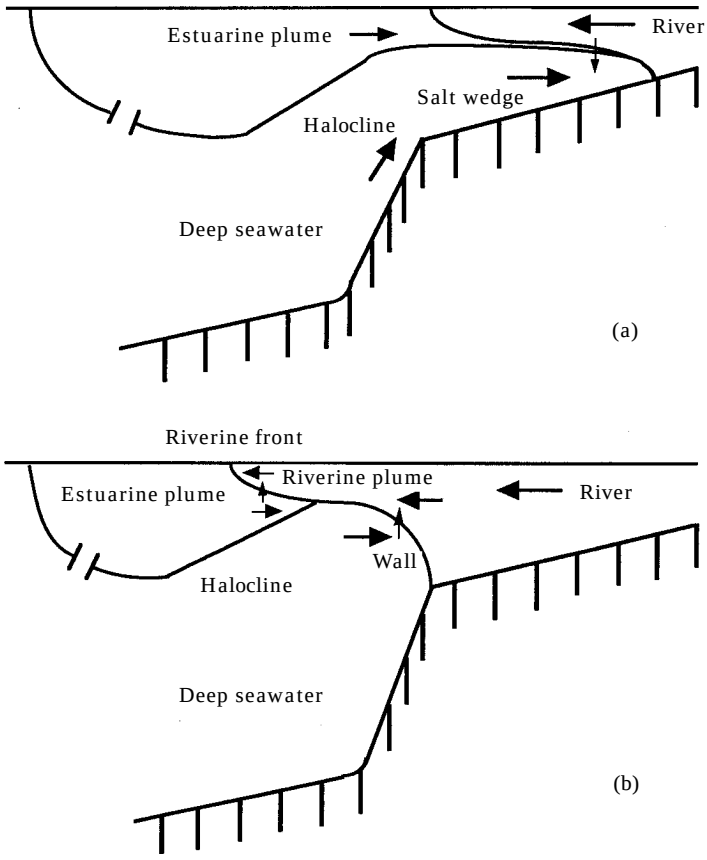

Figure 3. The conceptual model illustrating the riverine plume, the estuarine plume and the deep seawater: (a) a salt wedge invades the river during a flood tide and the estuarine plume dams the river outflow at the river mouth during higher high water (HHW), and (b) the riverine plume is formed as the salt wedge retreats during an ebb tide. A high salinity seawater wall-like structure is formed at the river mouth.

The transect started at the higher high water (HHW) on 13 August and ended 1·25 h after the lower low water (LLW) on 14 August (Figure 5). Stations R3 and R4 were also visited during a spring and neap tide in June 1989.

Transect results

Salinity, T-S diagram, proportion and equivalent thickness

Although spatial changes in vertical profiles along the transect shown in Figure 6 can not be separated from temporal changes due to tidal effects, they and their corresponding T-S diagrams (Figure 7) indicate the number of water masses present in the water column, how they are mixed relatively (Figure 8) and whether entrainment of NO_3 occurs.

The salinity profile in Figure 6 shows that the surface salinity increased downstream from R1 to station 2. The major halocline became shallower and sharper as one moved just outside the river mouth (R5) from both sides (from R1 to R4 and station 2 to R4).

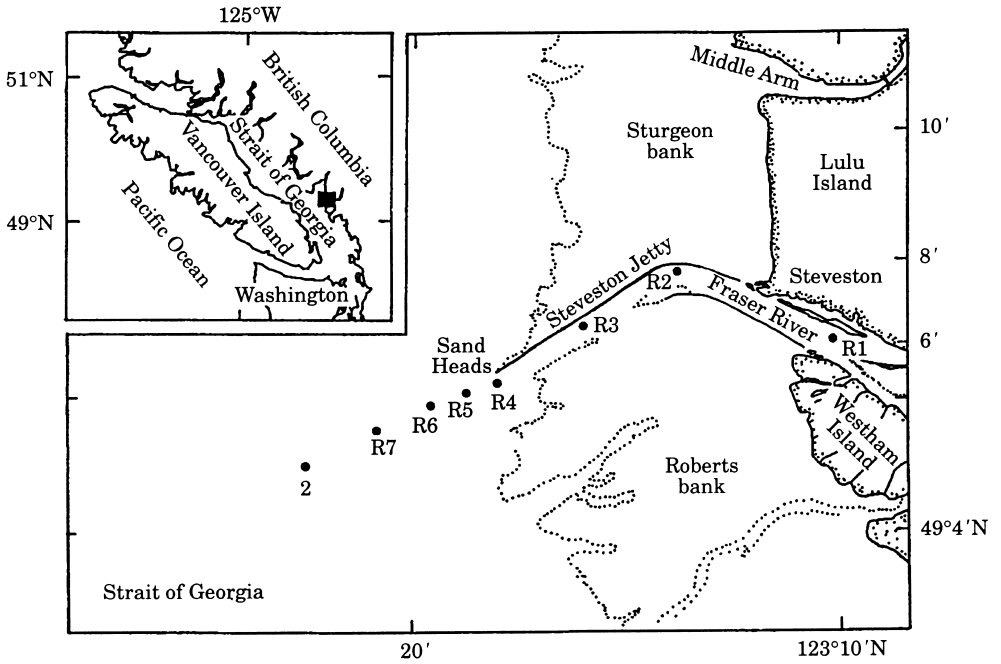

Figure 4. Map of the study area at the mouth of the Fraser River, British Columbia, Canada and the stations R1, R2, R3, R4, R5, R6, R7 and station 2 along the transect. Station depths: R1 = 15 m, R2 = 20 m, R3 = 12 m, R4 = 15 m, R5 = 45 m, R6 = 96 m, R7 = 146 m, station 2 = 200 m. The dotted line shows the edge of the shallow banks which are exposed at lower low water.

These changes were probably due to the sudden shoaling which results in the formation of the high-salinity wall at the river mouth as indicated in the conceptual model [Figure 3(b)]. There was a mixed layer (about 2 m thick) within the halocline at R2. Beyond the river mouth, the water column became multi-layered (R6, R7 and station 2; Figure 6). The T-S diagrams (Figure 7) show that the multi-layers consisted of different water masses. There were mainly three water masses. At R6, R7 and station 2, the line segment for salinity >27 is the water mass referred to as the deep seawater which was much less influenced by daily freshwater discharge. At R5, the straight line segment between the lowest salinity and medium salinity (15) indicates a water mass formed from the mixing of the freshwater and the water of the estuarine plume. This water mass is referred to as the riverine plume. The line between the medium salinity (14) and higher salinity (25) at R5 characterizes the estuarine plume water. The higher temperature at a salinity of 14 probably resulted from solar heating of the surface of the estuarine plume in the Strait of Georgia before the riverine plume spreads over it. Apparently, the temperature rise and the middle mixed layer at R2 indicated that the estuarine plume had invaded the river with the advance of the salt wedge. The T-S line became straighter at the river mouth as a result of intensive entrainment. There was direct contact between freshwater and the deep seawater allowing entrainment of NO_3.

One clear piece of evidence for entrainment of the deep seawater is that at R6 the surface temperature (16 °C) was lower than the river temperature of 17 °C, indicating entrainment of colder water during movement of the riverine plume.

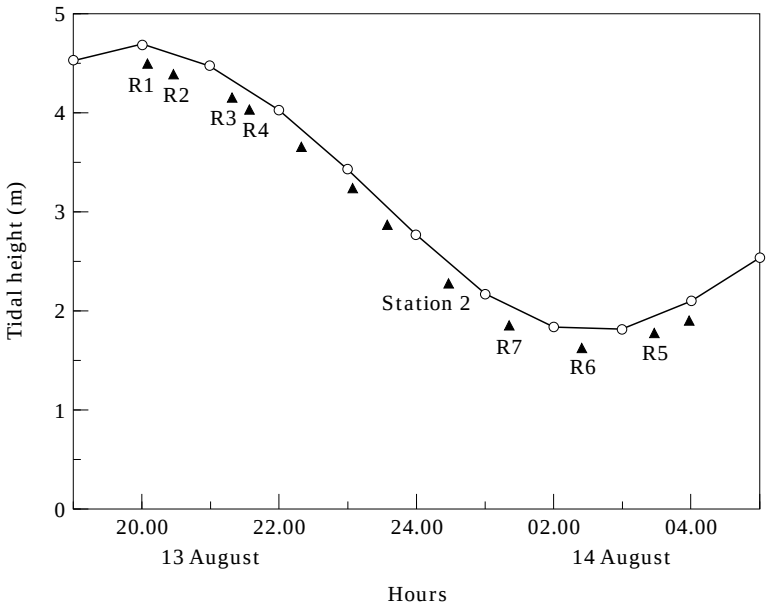

Figure 5. Change in tidal height with time during the sampling period along the transect on 13–14 August 1991. The arrows indicate the sampling times at which the stations were visited. Vertical profiles are shown in Figure 6 for those labelled stations only.

A T-S diagram can indicate how many water masses are present in the water column but it does not tell the volume of each water type. Figure 8 shows the vertical distribution of relative proportions of the freshwater, estuarine plume and deep seawater. The proportion of the freshwater and the depth to which the freshwater penetrated (proportion = 0) decreased downstream. The estuarine plume proportion at the river mouth at R4 was minimal along all the stations. It is worth pointing out that the proportion of the deep seawater at R6 (Figure 8) was higher at the surface (23%) than at 5 m (10%), corresponding to the colder temperature at the surface in the T-S diagram (Figure 7; R6). This is clear evidence for entrainment of deep seawater to the surface, and hence, an increase in NO_3 concentration was observed to occur at the surface at R6.

Nitrate

At R1, the surface NO_3 concentration was 3·2 μM (Figure 6) and it is taken to represent the NO_3 concentrations in the river water. The surface NO_3 value remained constant at 3·2 μM at R2, R3 and R4 in the river, while the deep water NO_3 increased from 13 μM at R1 to 25 μM at R4. Nitrate concentrations were undetectable at the surface at R7 and station 2, but were only 10–15 μM at 15 m. A unique feature in the vertical profiles of NO_3 was a minimum concentration at an intermediate depth at R5 and R6.

Entrainment of NO_3 was observed at R6 during the end of the ebb tide (Figure 6). The surface NO_3 concentration was 6 μM at R6 (Figure 6) which was twice as high as 3·2 μM in the river water. Surface NO_3 concentrations were 4·5 μM at R5. The question is, where did the increased NO_3 concentrations come from? Since NO_3 was undetectable in the surface estuarine plume (station 2 and R7), the potential sources of NO_3 were the

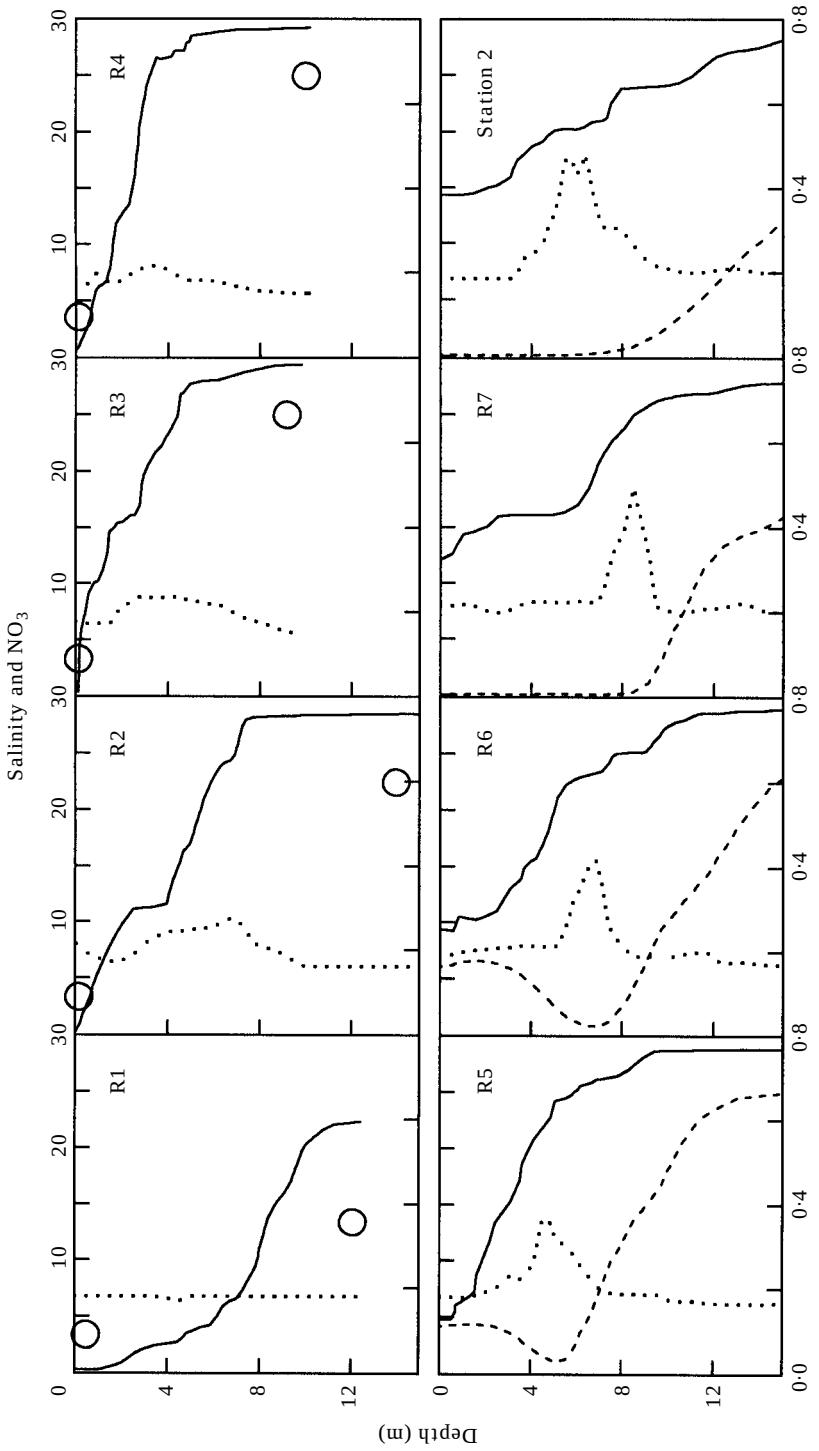

Figure 6. Vertical profiles of salinity (———), NO_3 (μM) (○ or – – –) and *in vivo* fluorescence (in relative units) (· · ·) at R1, R2, R3, R4, R5, R6, R7 and station 2 (Figure 4) along the transect on 13–14 August (Figure 5).

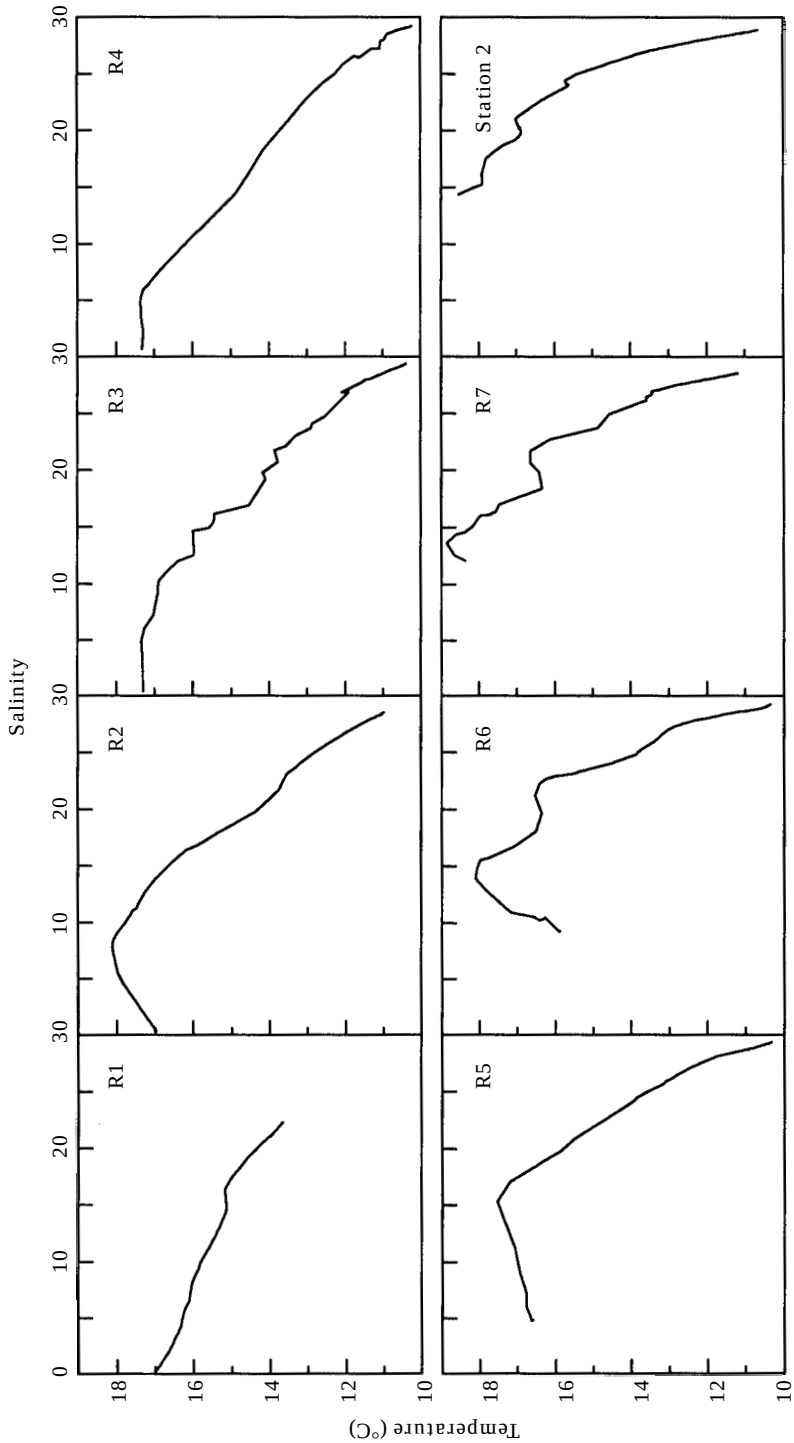

Figure 7. Temperature–salinity diagrams for the vertical profiles at the same stations along the transect as in Figure 4.

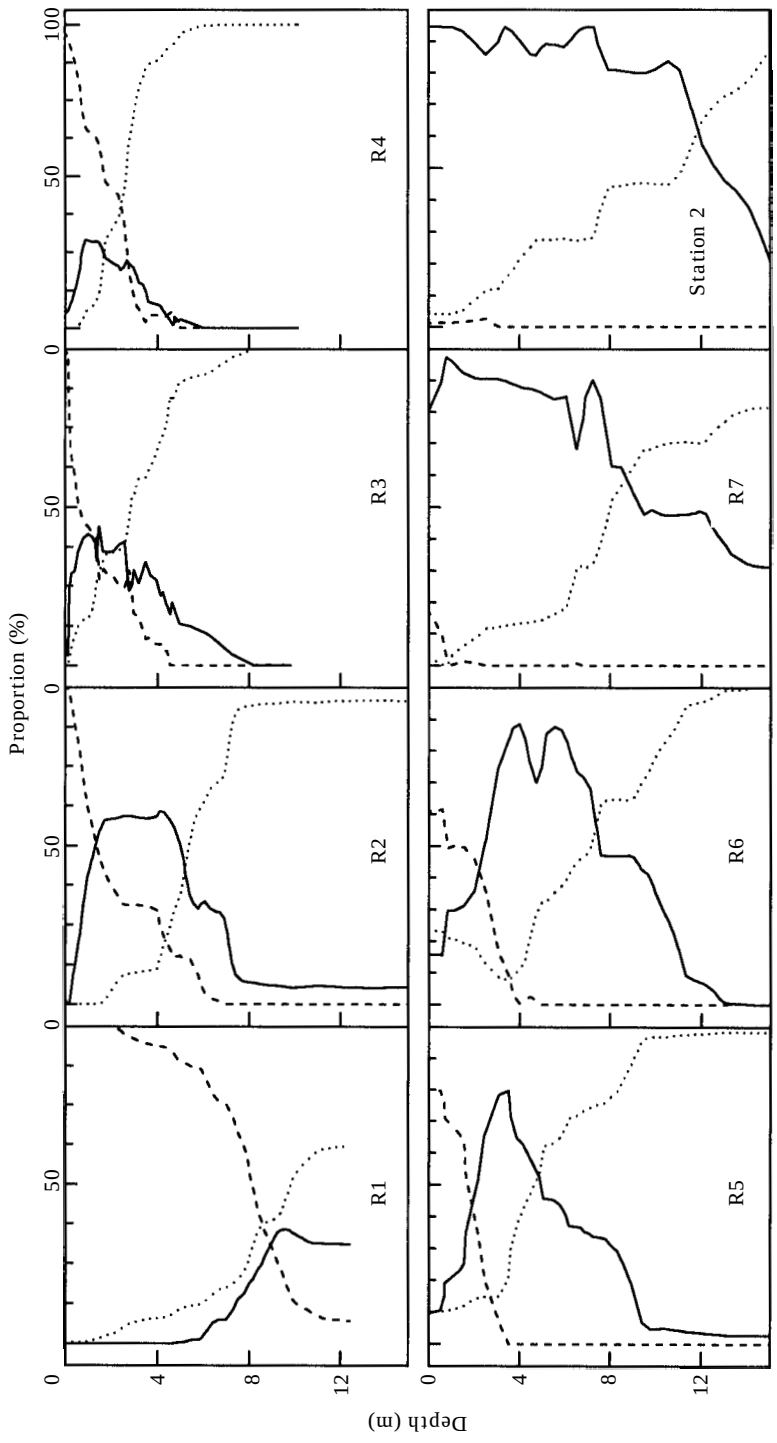

Figure 8. Vertical distribution of the proportions of the riverine plume (– – –), estuarine plume (———) and deep water (· · ·) for the vertical profiles at the same stations along the transect as in Figure 4.

river and the deep seawater. Nitrate concentrations were 3·2 μM in the river, and >10 μM in the deep seawater. Assuming no temporal changes in river NO_3 during such a short time, the only way to increase the surface NO_3 to a higher concentration than the river was from the deep seawater. However, there was a NO_3 minimum (lower than the river NO_3 concentration) between the riverine plume and the deep seawater at R6 and R5, which indicated that the increased NO_3 concentrations could not possibly occur through local vertical mixing at R6 and R5. Therefore, the higher NO_3 concentration observed at R6 must have been entrained from the deep NO_3-rich seawater closer to the river. However, one would expect that the surface NO_3 concentration at R5 would be higher than at R6, or that there would be no minimum NO_3 concentration at an intermediate depth at R5, because it would be decreased by dilution with the estuarine plume as the water moved from R5 to R6. The only reasonable explanation was the tidal phase change: R6 was sampled during the LLW, while R5 was sampled 1·25 h later. Current velocity in the river usually reaches a maximum shortly before LLW (Geyer & Farmer, 1989). When the outflow of the freshwater reached a maximum, the estuarine plume was pushed further seaward [Figure 3(b)]. At the same time, the outflow of the freshwater entrained some deep water and the amount of entrainment of NO_3 should be the largest at this time of the tidal cycle. When the outflow decreased, the amount of the entrained NO_3 decreased. The higher surface NO_3 concentration at R6 than at R5 could reflect this process.

From a T-S diagram, the amount of the entrained deep water expressed in equivalent thickness (m) can be calculated by the depth-integration of its vertical proportion distribution (Figure 8). The criterion for the entrained deep water (i.e. above which depth the deep water was considered to be ‘entrained’) was based on the depth (D_0) at which the proportion of the freshwater was 0%. In other words, above that depth (D_0) the deep seawater was the entrained (entrained deep seawater) and the estuarine plume was the entrained estuarine plume. The measured NO_3 concentrations were contributed by the three water types. However, the estuarine plume contained undetectable NO_3 at station 2. Therefore, NO_3 in the estuarine plume in the river channel was originally from the deep water and the freshwater. The measured concentrations minus the proportions of the river freshwater were NO_3 entrained from the deep water. When integrated from the surface to the same depth as the one (D_0) for the entrained deep water, the integrated NO_3 was the amount of the entrained NO_3.

At R6 where the increased NO_3 concentration was seen, the calculated entrained NO_3 was 19·5 mmol m^{-2} and the equivalent thickness of the entrained deep water was 0·65 m [Figure 9(a)]. At R5, the entrained NO_3 was 9·1 mmol m^{-2} with 0·46 m equivalent thickness of the entrained deep water. However, at station 2 and R7, there was no entrained deep water and no entrained NO_3 either. The relationship between the entrained deep water and the entrained NO_3 is shown in Figure 9(a). The regression analysis indicated a significant dependence of the entrained NO_3 on the entrained deep water ($R^2 = 0{\cdot}90$).

Fluorescence maximum

One persistent feature in fluorescence at all the stations was a fluorescence maximum present in all the vertical profiles except R1 (Figure 6). It was located at the bottom of the halocline or the interface between the estuarine plume and the deep water. The

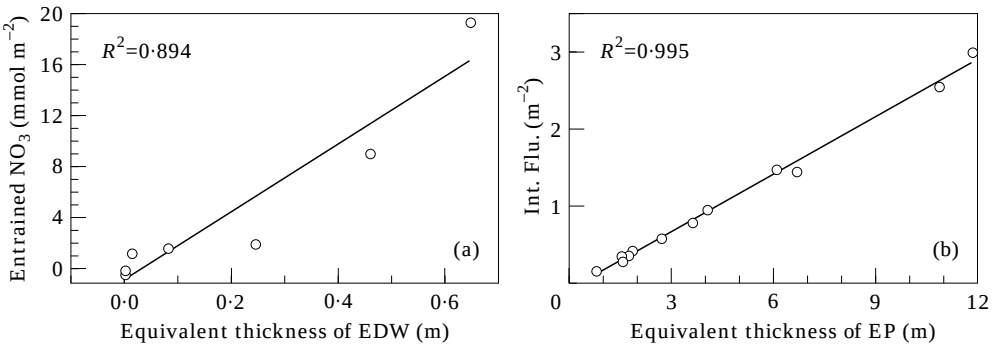

Figure 9. Dependence of (a) depth-integrated entrained NO_3 on entrained deep seawater (EDW), and (b) depth-integrated fluorescence (Int. Flu.) in the water column on the equivalent thickness of the estuarine plume (EP), for the vertical profiles at the same stations along the transect as in Figure 4, on 13–14 August 1991.

maximum moved up and down with the depth of the interface and its thickness also appeared to vary with the interface thickness. It is reasonable to assume that phytoplankton in the fluorescence maximum originally grew in the estuarine plume away from the river mouth. Although the mechanisms are yet to be studied, the observed fluorescence could be mainly accounted for by the volume of the estuarine plume in the water column, if mixing processes had shorter time-scales than changes in chlorophyll fluorescence due to biological processes such as consumption by heterotrophic organisms and the *in situ* growth (Harris, 1980).

Regression analysis indicates that an integration of the fluorescence contributed by the estuarine plume over the water column is strongly linearly related with the equivalent thickness of the estuarine plume [R^2=0·995; Figure 9(b)]. This strong relationship indicated that the fluorescence maximum was formed in the estuarine plume away from the river mouth and advected into the river with the salt wedge. The fluorescence distribution was a result of mixing of the estuarine plume with the riverine plume and the deep seawater since mixing was much faster than the biological processes.

Figure 10 shows uptake of nutrients incubated at different irradiances for a sample taken at the fluorescence maximum at station 2. The sample depth was below the 1% light depth. No nutrients were added to the samples. There was no or little uptake of nutrients in the dark. However, it is possible that those cells might have taken up nutrients rapidly when first brought to the nutrient-rich water and become internally saturated. When the samples were incubated at a range of irradiances, the uptake increased with increasing irradiance. The response clearly shows that phytoplankton at the chlorophyll *a* maximum did possess the potential to increase their nutrient uptake when exposed to improved light conditions.

Effects of tides on entrainment

Observations were made at R3 and R4 during flood and ebb tides during both spring and neap tides in June 1989. Figure 11 shows the change in the tidal height with time and the sampling times at R3 and R4 for the spring and neap tides.

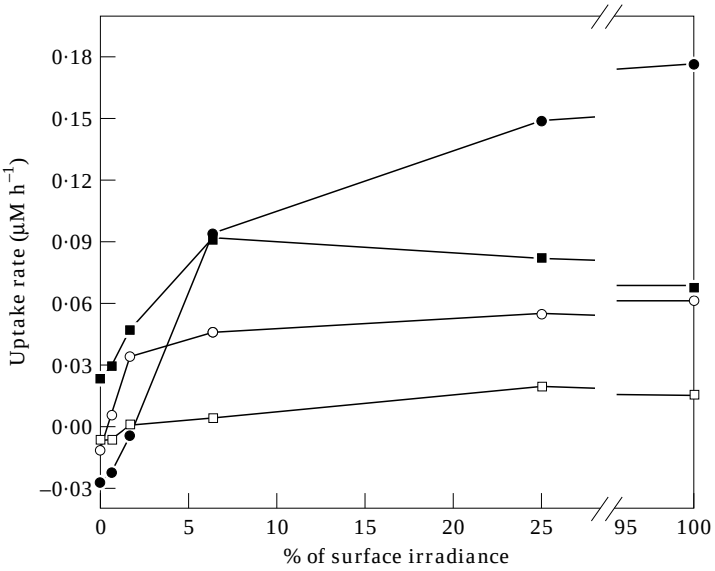

Figure 10. Uptake of nutrients over a range of irradiances for a sample taken at the chlorophyll *a* maximum at 10 m at station 2 on 12 June 1989. The initial concentrations of nutrients were saturating (NO_3 = 7·9 μM, SiO_4 = 13·0 μM, NH_4 = 1·32 μM, and PO_4 = 1·5 μM). ●, NO_3; ■, SiO_4; ○, NH_4; □, PO_4.

Neap tide

Flood. Although the sampling times were just after low water, the following observations indicated the status of a flood tide. At R3 inside the river, a surface mixed layer was absent (Figure 12; R3–A1), suggesting that a salt wedge had moved into (or still stayed in) the river and entrained freshwater downwards, which is consistent with the conceptual model [Figure 3(a)] and a previous study (Geyer & Farmer, 1989). The T-S diagram shows that the estuarine plume was present, but no longer a distinct water body (Figure 12; R3–A2). At R4, the river mouth, there was only a very thin riverine plume, indicating that the estuarine plume was pushed to the river mouth (Figure 12; R4–A1). The estuarine plume is distinctly shown as the ‘knee’ at salinity of 22 in the T-S diagram (Figure 12; R4–A2).

Ebb. When the tidal height approached LLW during the following ebb, the vertical profile (Figure 12; R3–B1) looked very similar to one during the flood (R3–A1). However, the T-S diagram is almost linear (Figure 12; R3–B2), indicating that the freshwater outflow was so strong that the estuarine plume was washed away at R3. At the same time, the freshwater outflow had started to entrain the deep water, as indicated by the cooler temperature at the surface during the ebb (Figure 12; R3–B2) than during the flood at R3 (Figure 12; R3–A2). The slope of the left line segment of the T-S diagram (R4–B2) points to the deep water (the lower-right end of the line), which indicates that freshwater had been mixed by entrainment with the deep water upstream initially and advected over the estuarine plume. The rise in temperature at a salinity of about 27 on the T-S diagram indicated the presence of the nutrient-poor estuarine plume, which could still be a barrier to nutrient entrainment as it lay between the riverine plume and the deep water at R4 during the neap tide ebb.

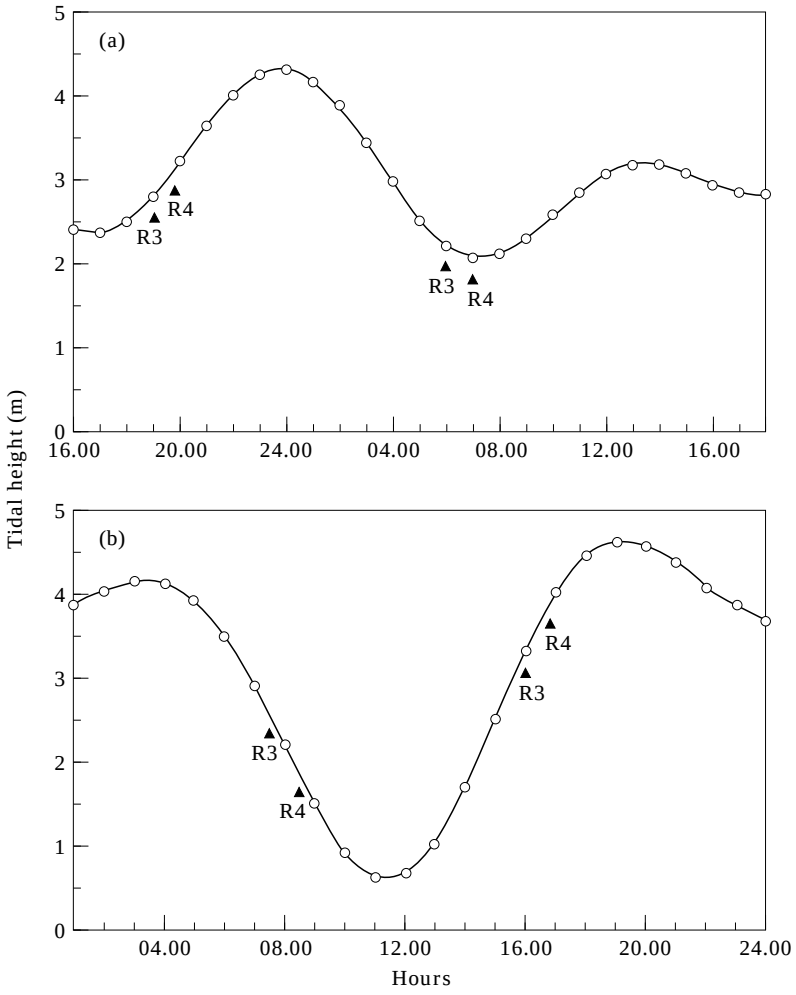

Figure 11. Change of the tidal height with time for (a) the neap tide on 11–12 June and (b) the spring tide on 19 June 1989. The arrows indicate the sampling times at which the vertical profiles were taken for Figures 12 and 13.

Spring tide

Flood. In the middle of the halocline (Figure 13; R3–A1), there was a layer where the salinity changed slowly; this layer was the estuarine plume being eroded between the freshwater and the deep water. This remnant of the estuarine plume can be seen in the T-S diagram (Figure 13; R3–A2) where there is a temperature rise at a salinity of 13 at which the eroded layer began in the vertical profile. At R4, the freshwater was completely absent and the estuarine plume was completely dominant in the top 4 m.

Ebb. At R3 during the ebb, there was a 2-m thick, surface mixed layer of nearly freshwater and very broad halocline (8 m) (Figure 13; R3–B1). The T-S curve shows only one straight line (Figure 13; R3–B2), indicating no estuarine plume. At R4, the halocline started at the surface (R4–B1) and the T-S line was also straight (Figure 13; R4–B2).

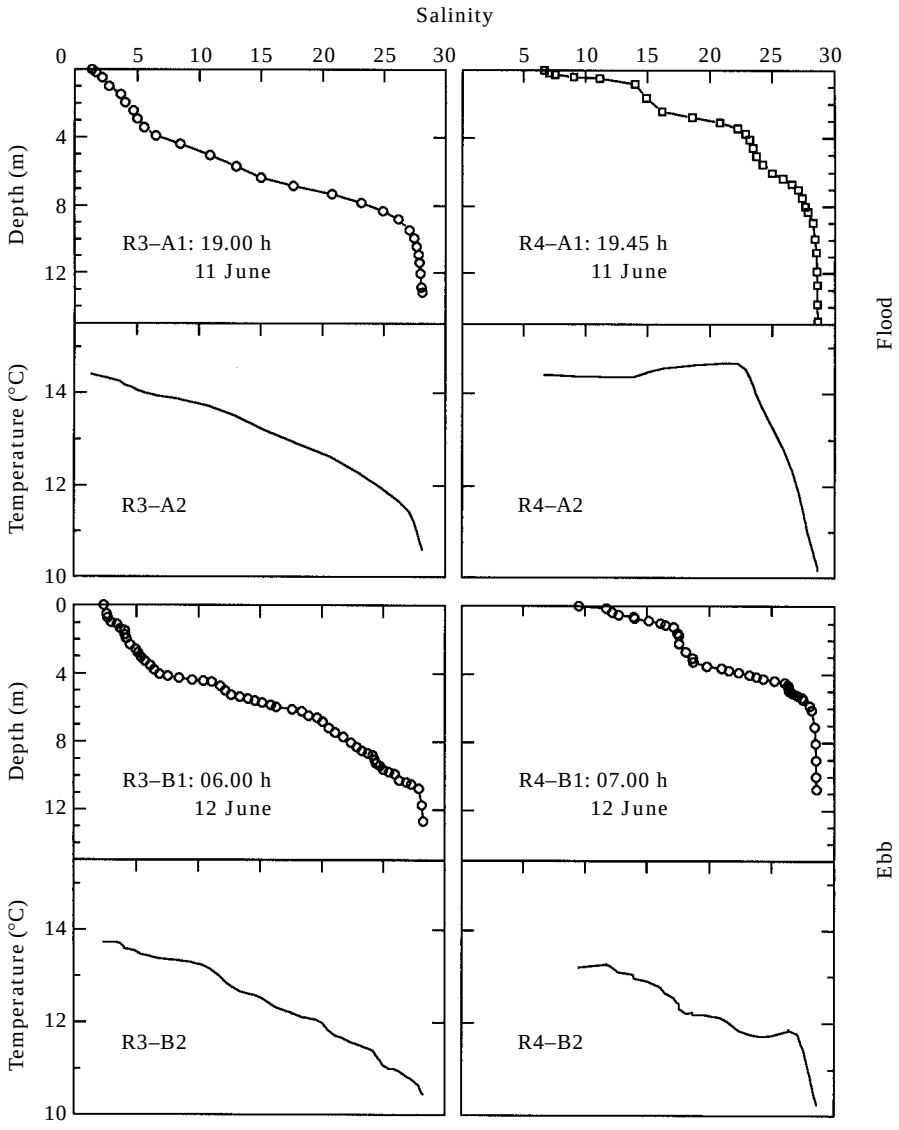

Figure 12. Vertical salinity profiles with their corresponding T-S diagrams at R3 and R4 during the flood and ebb of the neap tide on 11–12 June 1989.

Comparison between the spring and neap tides

The vertical distribution of the proportion of freshwater, the estuarine plume and the deep water for the vertical profiles during the spring and neap tides are shown in Figure 14. It is apparent that the estuarine plume occupied a larger proportion of the water column at R4 than at R3 during the same tidal stages, and a larger proportion during flood tides than during ebb tides, but less during the spring ebb than the neap ebb at the same station. The sampling times during the spring tide were only in the middle of the ebb compared with the end of neap ebb, suggesting that during LLW of the spring ebb, there would be even more entrainment of deep water.

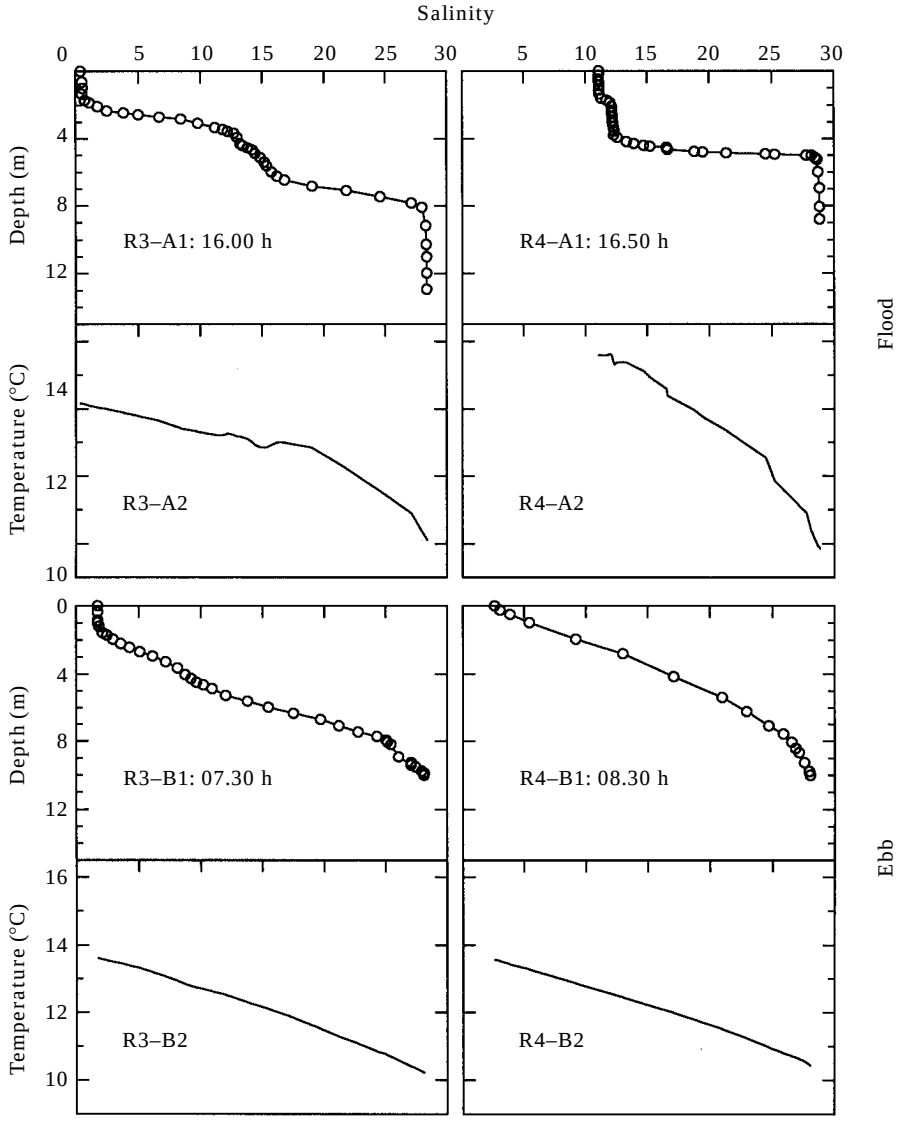

Figure 13. Same as Figure 12 except during the spring tide on 19 June 1989.

In general, during a flood, the freshwater outflow slows down in the river during the salt wedge invasion carrying the estuarine plume. During an ebb when the salt wedge retreats, the freshwater outflow increases and pushes the estuarine plume downstream. At the same time, deep seawater was entrained. When the tidal range is small during the neap tide, the estuarine plume is hardly pushed out of the river during the ebb tide (Geyer & Farmer, 1989). During the spring tide, however, the estuarine plume is completely washed out of the river during the ebb. The decrease in the estuarine plume volume results in more direct contact between the two water masses, freshwater and deep seawater, and more entrainment of deep water into the river outflow.

There was a significant dependence ($P = 0{\cdot}05$) of the entrained deep water on the amount of the estuarine plume present in the water column (note: different from

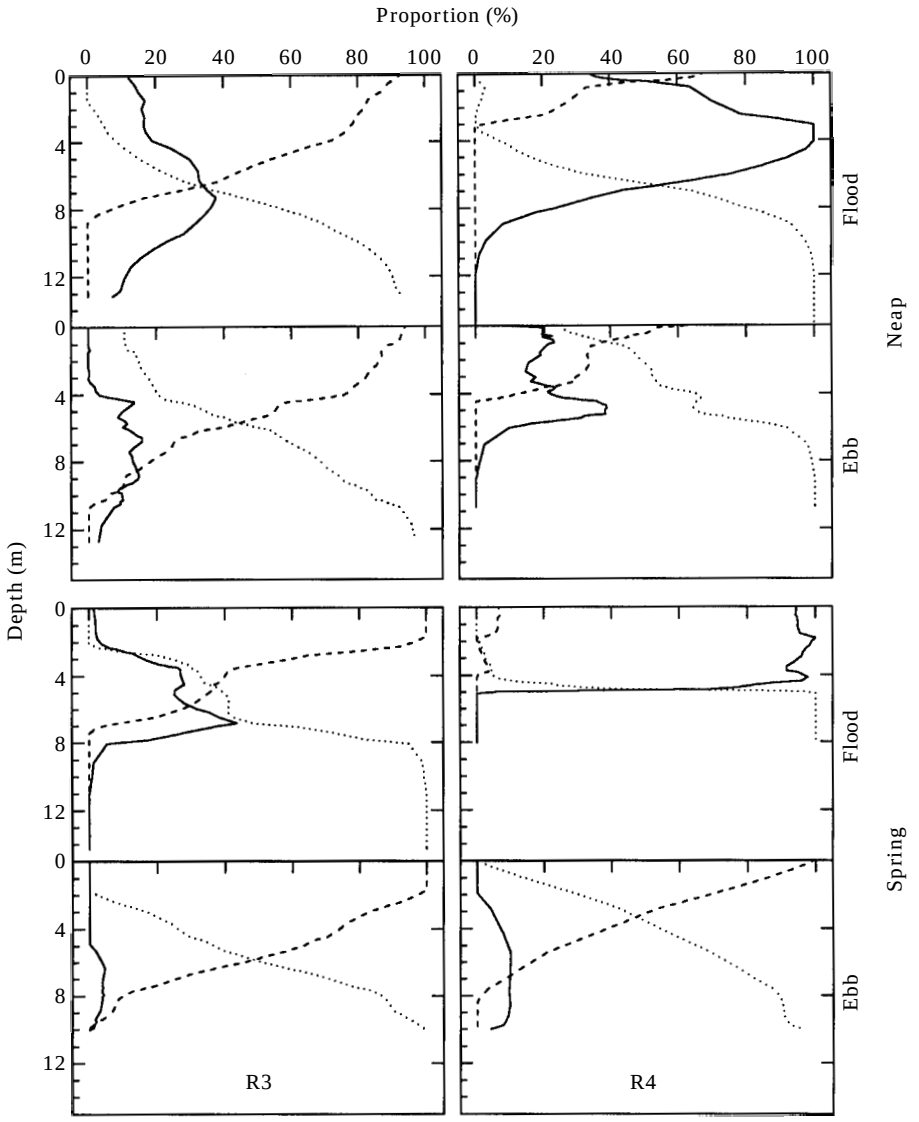

Figure 14. Vertical distribution of the proportion of freshwater (– – –), the estuarine plume (———) and the deep water (· · ·) for the vertical profiles at R3 and R4 during the neap tide (11–12 June) shown in Figure 12 and during the spring tide (19 June 1989) shown in Figure 13.

the entrained estuarine plume) and it was supported by the regression analyses for the transect on 13–14 August 1991 ($R^2 = 0{\cdot}73$), for the neap tide ($R^2 = 0{\cdot}84$) and for the spring tide ($R^2 = 0{\cdot}68$; Figure 15). Furthermore, the slope during the spring tide is steeper than the slope during the neap tide (Figure 15), indicating that a smaller variation in the thickness of the estuarine plume resulted in a larger change in the amount of the deep water. These results suggest that there was more entrainment of NO_3 during the spring tide than during the neap tide, although NO_3 concentrations were not available to estimate direct entrainment of NO_3.

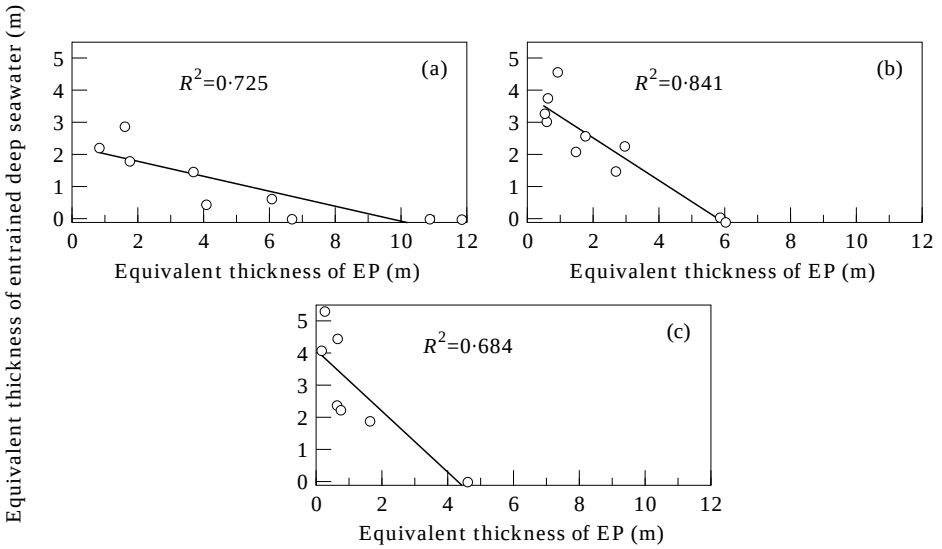

Figure 15. The relationship between the equivalent thickness of the entrained deep water (EDW) and the equivalent thickness of the estuarine plume (EP) for the vertical profiles: (a) along the transect on 13–14 August 1991, (b) at R3 and R4 during the neap tide on 11–12 June 1989, and (c) at R3 and R4 during the spring tide on 19 June 1989. Some vertical profiles shown in Figure 4 are not included in (a) because they were not deep enough for the calculation of the equivalent thickness of the estuarine plume.

Also, because a neap tide is usually preceded by pre-neap tides in the similar ranges, the salt wedge may not be washed out of the river. Thus, during the neap tide, some of the estuarine plume water would remain in the river and partially mix with the deep water (Figure 12). In contrast, during the spring tide the estuarine plume is flushed out of the river as is shown in the T-S diagrams (Figure 13). As a result, the source NO_3 concentrations in the deep water would be more diluted by the estuarine plume water during the neap tide. This dilution was shown at R1 (Figure 6) where the bottom mixed layer had a salinity of 22 and a NO_3 concentration of 13 μM, lower than the expected 17 μM for that salinity (22) if mixing only occurred between the freshwater (3·2 μM) and the deep water of salinity 30 (25 μM) (assuming conservative mixing). The reduced NO_3 concentration will make a great difference in NO_3 entrainment even when the amount of the entrained deep water is similar. The difference in entrainment between the spring and neap tides will be discussed in the time series at station 2 (Yin *et al.*, 1995*a*).

Biological significance

Studies of nutrient dynamics associated with entrainment are sparse. The best documented case is that of the St Lawrence estuary. The Laurentian Channel shoals in the lower estuary up to the entrance of Saguenay Fjord. The intermediate layer in the channel is cold and nutrient-rich water moves upstream in the residual circulation. The intensity of upstream currents in the intermediate layer was proportional to freshwater runoff (Ingram, 1979). The surface layer waters from the upper estuary and the Saguenay Fjord flow downstream. As a result, intensive upward entrainment of the intermediate layer occurs at the head of the channel. Flood tides literally lift the water

column along the abrupt rise in the Laurentian Channel topography, such that intermediate cold water spills over the shallow mid-channel area (Reid, 1977). During ebb tides, the upwelled cold waters are mixed and flushed downstream. As a result, relatively cold waters are found at the surface near the head of the lower St Lawrence estuary, which was observed from a satellite thermal image of the region (Gratton *et al.*, 1988). Temperature and salinity distribution at the head shows that isopycnals are periodically advected towards the surface by incoming tides (Ingram, 1975; Therriault & Lacroix, 1976; Greisman & Ingram, 1977). This entraining process has been called a ‘nutrient pump’ (Steven, 1974) and enhances biological production in the Gaspé Current downstream (see review by de Lafontaine *et al.*, 1991). The nutrient source from the seawater origin represents 75% of the total nutrient supply to the euphotic zone in the estuary, while the freshwater origin contributes only <25% (de Lafontaine *et al.*, 1991).

In the Fraser River estuary, because of the presence of the estuarine plume in the middle between the freshwater layer and the deep seawater layer, the freshwater outflow first entrains the estuarine plume water away before it reaches the deep seawater. Entraining high NO_3 probably occurs later, after the estuarine plume is washed away. The chlorophyll *a* maximum at the base of the estuarine plume is a common feature in this system although the formation mechanism is yet to be studied. Phytoplankton in the maximum are advected towards the river and a portion of them enter the river channel with the estuarine plume as the salt wedge invades during flood tides. As the river outflow starts during ebb tides, phytoplankton are entrained upwards and advected seaward. Some marine phytoplankton cells may die if the salinity is lower than their tolerance. The entrained phytoplankton will be in the upper layer in the Strait after they have left the river channel. By then, they must be internally nutrient saturated since these phytoplankton at the base of the estuarine plume have been exposed to nutrients in the deep water before they are advected to the river and are exposed to nutrients during the entraining processes. They may serve as seed phytoplankton populations and grow, possibly developing blooms further seaward when they gradually become part of the estuarine plume, and utilize the riverine nutrients and the entrained nutrients along with improved light conditions. Part of the phytoplankton may sink and join the chlorophyll maximum at the base of the estuarine plume. The chlorophyll maximum might be carried towards the river again, starting another cycle. This process occurs during the tidal cycle and provides nutrients to the euphotic zone periodically. This process may be related to the maximum in primary productivity which was shown in the estuarine plume (Parsons *et al.*, 1969; Stockner *et al.*, 1979). It may also be a reason for zooplankton to aggregate at the riverine front (Mackas & Louttit, 1988) and to be abundant in the estuarine plume (St John *et al.*, 1992).

Acknowledgements

We thank Dr Mike St John and Peter Clifford who coordinated the cruises, and David Jones for helping to set up the vertical profiling system. Thanks are given to the Department of Fisheries and Oceans for providing ship time, and the officers and crew of C.S.S. *Vector* for their assistance. Discussions with Dr Keith Thomsen were helpful and comments by Drs James Cloern, Peter Frank and Ken Denman improved the manuscript.

This research was funded by a Natural Sciences and Engineering Research Council of Canada (NSERC) Strategic grant. The Research Fellowship to support K. Yin was kindly provided by the Department of Fisheries and Oceans, Pacific Biological Station, Nanaimo, British Columbia, Canada.

References

Ages, A. & Woollard, A. 1988 Tracking a pollutant in the lower Fraser River: a computer simulation. *Water Pollution Research Journal of Canada* **23,** 122–140.

Armstrong, F. A. J., Stearns, C. R. & Strickland, J. D. H. 1967 The measurement of upwelling and subsequent biological processes by means of the Technicon AutoAnalyzer and associated equipment. *Deep-Sea Research* **14,** 381–389.

Brandt, A., Sarabun, C. C., Seliger, H. H. & Tyler, M. A. 1987 The effects of the broad spectrum of physical activity on the biological processes in the Chesapeake Bay. In *Proceedings of the 17th International Liege. Colloq. on Ocean Hydrodynamics: Dynamic Biological Processes at Marine Interfaces*, pp. 361–384.

Clifford, P. J., Cochlan, W. P., Harrison, P. J., Yin, Y., Sibbald, M. J., Albright, L. J., St John, M. A. & Thompson, P. A. 1989 Plankton production and nutrient dynamics in the Fraser River plume, 1987. *Department of Oceanography, University of British Columbia Report* No. 51. 118 pp.

Clifford, P. J., Harrison, P. J., Yin, K., St John, M. A., Waite, A. M. & Albright, L. J. 1990 Plankton production and nutrient dynamics in the Fraser River plume, 1988. *Department of Oceanography, University of British Columbia Report* No. 53. 142 pp.

Clifford, P. J., Harrison, P. J., St John, M. A., Yin, K. & Albright, L. J. 1991 Plankton production and nutrient dynamics in the Fraser River plume, 1989. *Department of Oceanography, University of British Columbia Report* No. 54. 255 pp.

Cordes, R. E., Pond, S., de Lange Boom, B. R., LeBlond, P. H. & Crean, P. B. 1980 Estimates of entrainment in the Fraser River Plume, British Columbia. *Atmosphere-Ocean* **18,** 15–26.

Drinnan, R. W. & Clark, M. J. R. 1980 Water chemistry: 1970–1978. Fraser River Estuary Study, Water Quality Working Group, Ministry of Environment, Parliament Buildings, Victoria, B.C., 150 pp.

Geyer, W. R. & Farmer, D. M. 1989 Tide-induced variation of the dynamics of a salt wedge estuary. *Journal of Physical Oceanography* **19,** 1060–1072.

Gratton, Y., Mertz, G. & Gagné, J. A. 1988 Satellite observations of tidal upwelling and mixing in the St Lawrence Estuary. *Journal of Geophysical Research* **93,** 6947–6954.

Greisman, P. & Ingram, G. 1977 Nutrient distribution in the St Lawrence Estuary. *Journal of the Fisheries Research Board of Canada* **34,** 2117–2123.

Hager, S. W., Gordon, L. I. & Park, P. K. 1968 A practical manual for the use of the Technicon Autoanalyzer in seawater nutrient analysis. *B.C.F. Report*, October 1968, Reference 68–73.

Harris, G. P. 1980 Temporal and spatial scales in phytoplankton ecology. Mechanisms, methods, and management. *Canadian Journal of Fisheries and Aquatic Science* **37,** 877–900.

Harrison, P. J., Fulton, J. D., Taylor, F. J. R. & Parsons, T. R. 1983. Review of the biological oceanography of the Strait of Georgia: pelagic environment. *Canadian Journal of Fisheries and Aquatic Science* **40,** 1064–1094.

Harrison, P. J., Clifford, P. J., Cochlan, W. P., Yin, Y., St John, M. A., Thompson, P. A., Sibbald, M. J. & Albright, L. J. 1991 Nutrient and phytoplankton dynamics in the Fraser River plume, Strait of Georgia, British Columbia. *Marine Ecology Progress Series* **70,** 291–304.

Ingram, R. G. 1975 Influence of tidally-induced vertical mixing on primary productivity in the St Lawrence Estuary. *Memorial Society Royale Science Liéges* **7,** 59–74.

Ingram, R. G. 1979 Water masses modification in the St Lawrence Estuary. *Naturaliste Canada* **106,** 45–54.

Jones, D. M., Harrison, P. J., Clifford, P. J., Yin, K. & St John, M. A. 1991 A computer-based system for the acquisition and display of continuous vertical profiles of temperature, salinity, fluorescence and nutrients. *Water Research* **25,** 1545–1548.

Kostaschuk, R. A. & Atwood, L. A. 1989 River discharge and tidal controls on salt-wedge position and implications for channel shoaling: Fraser River, British Columbia. *Canadian Journal of Civil Engineering* **17,** 452–459.

de Lafontaine, Y., Demers, S. & Runge, J. 1991 Pelagic food web interactions and productivity in the Gulf of St Lawrence: a perspective. In *The Gulf of St Lawrence: Small Ocean or Big Estuary*? (Therriault, J.-C., ed.). *Canadian Special Publication in Fisheries and Aquatic Science* **113,** 99–123.

Mackas, D. L. & Louttit, G. C. 1988 Aggregation of the copepod *Neocalanus plumchrus* at the margin of the Fraser River plume in the Strait of Georgia. *Bulletin of Marine Science* **43,** 810–824.

Mann, K. H. & Lazier, J. R. N. 1991 *Dynamics of Marine Ecosystems: Biological–Physical Interactions in the Oceans*. Blackwell Scientific Publications, Boston, 466 pp.

Parsons, T. R., LeBrasseur, R. J., Fulton, J. D. & Kennedy, O. D. 1969 Production studies in the Strait of Georgia. I. Primary production under the Fraser River plume, February to May, 1967. *Journal of Experimental Marine Biology and Ecology* **3,** 27–38.

Parsons, T. R., Albright, L. J. & Parslow, J. 1980 Is the Strait of Georgia becoming more eutrophic? *Canadian Journal of Fisheries and Aquatic Science* **37,** 1043–1047.

Pickard, G. L. & Emery, W.J. 1982 *Descriptive Physical Oceanography: an Introduction*. 4th edn. Pergamon Press, Oxford, 249 pp.

Pond, S. & Pickard, G. L. 1978 *Introductory Dynamic Oceanography*. Pergamon Press, Toronto, 241 pp.

Reid, S. D. 1977 Circulation and mixing the St Lawrence estuary near Ilet Rouge. *Bedford Institute of Oceanography* (*Dartmouth*) *Report* No. BI-R-77. 36 pp.

St John, M. A., Macdonald, J. S., Harrison, P. J., Beamish, R. J. & Choromanski, E. 1992 The Fraser River plume: effects on the distribution of juvenile salmonids, herring and their prey. *Fisheries Oceanography* **1,** 153–162.

Slawyk, G. & MacIsaac, J. J. 1972 Comparison of two automated ammonium methods in a region of coastal upwelling. *Deep-Sea Research* **19,** 521–524.

Steven, D. M. 1974 Primary and secondary production in the Gulf of St Lawrence. *McGill University, Marine Science Centre Report* No. 26. 116 pp.

Stockner, J. G., Cliff, D. D. & Shortreed, K. R. S. 1979 Phytoplankton ecology of the Strait of Georgia, British Columbia. *Journal of the Fisheries Research Board of Canada* **36,** 657–666.

Stronach, J. A. 1981 The Fraser River plume, Strait of Georgia. *Ocean Management* **6,** 201–221.

Therriault, J.-C. & Lacroix, G. 1976 Nutrients, chlorophyll, and internal tides in the St Lawrence Estuary. *Journal of the Fisheries Research Board of Canada* **33,** 2747–2757.

Waldichuk, M. 1957 Physical oceanography of the Strait of Georgia, British Columbia. *Journal of the Fisheries Research Board of Canada* **14,** 321–486.

Wood, E. D., Armstrong, F. A. J. & Richards, F. A. 1967 Determination of nitrate in seawater by cadmium–copper reduction to nitrite. *Journal of the Marine Biological Association of the United Kingdom* **47,** 23–31.

Yin, K., Harrison, P. J., Pond, S. & Beamish, R. J. 1995*a* Entrainment of nitrate in the Fraser River estuary and its biological implications. II. Effects of spring *vs.* neap tides and river discharge. *Estuarine, Coastal and Shelf Science* **40**, 529–544.

Yin, K., Harrison, P. J., Pond, S. & Beamish, R.J. 1995*b* Entrainment of nitrate in the Fraser River estuary and its biological implications. III. Effects of winds. *Estuarine, Coastal and Shelf Science* **40,** 545–558.